IOP Publishing New J. Phys. 26 (2024) 103011 https://doi.org/10.1088/1367-2630/ad817f

New Journal of Physics
The open access journal at the forefront of physics

Deutsche Physikalische Gesellschaft DPG
IOP Institute of Physics

Published in partnership with: Deutsche Physikalische Gesellschaft and the Institute of Physics

OPEN ACCESS

RECEIVED
12 July 2024

REVISED
19 September 2024

ACCEPTED FOR PUBLICATION
30 September 2024

PUBLISHED
10 October 2024

PAPER

Experimental determination of the sulfur K-shell fundamental parameters employing the holistic approach

Philipp Hönicke

Helmholtz-Zentrum Berlin (HZB), Hahn-Meitner-Platz 1, 14109 Berlin, Germany
Physikalisch-Technische Bundesanstalt (PTB), Abbestr. 2-12, 10587 Berlin, Germany

E-mail: philipp.hoenicke@helmholtz-berlin.de

Keywords: x-ray fluorescence, sulfur, K-shell fluorescence yield, transition probabilities, fundamental parameters

Abstract

Sulfur and its compounds are both very abundant in the environment and very important for technological applications such as batteries. X-ray spectroscopic characterizations of sulfur compounds for a quantitative determination of the present amount of sulfur often requires a good knowledge on the atomic fundamental parameters involved. These quantitatively describe the processes of photoionization and x-ray fluorescence emission, making them crucial for x-ray spectroscopy-based quantifications. By employing the recently demonstrated holistic approach, the atomic fundamental parameters of the sulfur K-shell were experimentally determined using the radiometrically calibrated instrumentation of the Physikalisch-Technische Bundesanstalt. The transition probabilities of the main K-shell fluorescence lines, the K-shell fluorescence yield, the K-shell Auger yield, the subshell photoionization cross section and fluorescence production cross section were determined by means of photon energy dependent x-ray fluorescence and transmission measurements on a thin InS coated silicon nitride membrane. The results are also downloadable from Zenodo as plain text.

1. Introduction

Sulfur is one of the most abundant elements and is used in various application fields. This includes agricultural aspects [1], medical applications [2], food production [3], rubber vulcanization [4, 5]. A very prominent application field for sulfur and sulfur containing materials is in electrochemical energy storage. Due to an operating voltage range of 2.1 V as well as a theoretical specific capacity of 1675 $\frac{\mathrm{mAh}}{\mathrm{g}}$, lithium-sulfur rechargeable batteries are superior with respect to cost and safety as compared to other battery cathode materials [6]. Especially in the field of sulfur containing batteries, x-ray spectroscopy (XRS) is highly relevant to increase the understanding of capacity fading and other aging mechanisms [7]. Atomic fundamental parameter based or even reference-free quantification [8] of x-ray fluorescence can help in this context to reveal structure performance relationships. And also in other fields, an XRS based quantification of sulfur is needed [9].

A reliable knowledge on the relevant atomic fundamental parameters (FP), such as fluorescence yields or photoionization cross-sections, is crucial for accurate quantitative analysis in x-ray fluorescence (XRF) in any of the aforementioned applications. Both, the accuracy and the precision of the employed FP data directly affects the results obtained. Thus, a reliable knowledge about the FP data, in this case for sulfur is crucial for such studies. However, much of the existing experimental FP data in literature is very old, only interpolated from adjacent elements, or purely theoretical without experimental validation. Furthermore, the uncertainties associated with these tabulated FP data are often unknown or only approximated [10]. To address this issue, initiatives such as the International initiative on x-ray fundamental parameters (FPI) [11] are revisiting and enhancing FP databases through new experiments [12, 13] and new advanced calculations [14]. Calibrated instrumentation [15] is utilized at the Physikalisch-Technische Bundesanstalt (PTB), to conduct dedicated experiments aimed at either evaluating existing or updating FP data [16–18]. Recently, an

updated holistic experimental and data evaluation procedure [19, 20] for an improved experimental FP determination has been developed to further reduce the achieveable experimental uncertainties and to expand the amount of accessible FPs. In this work, this approach is applied to sulfur in order to determine relevant FPs for the sulfur K-shell such as the fluorescence yield, the sulfur K-shell photo ionization cross sections and other FPs. With respect to previous works related to the sulfur K-shell FPs, the holistic approach provides a more thorough insight, both in terms of the achievable uncertainties and for most of the relevant FPs. All results are also downloadable from Zenodo as plain text [21].

2. Experimental section

For an experimental determination of the sulfur K-shell fundamental parameters, one needs to record both, the transmission and the sulfur K-shell x-ray fluorescence emission of either a free standing foil or a thin coating on e.g. a silicon nitride membrane. The mass thickness (a product of material density and thickness) must be carefully chosen so that the sample transmission in the studied photon energy range remains between 5% and 95%, ensuring reliable data [22]. As it is not straightforward to use a mono elemental sulfur thin foil or coating, an InS_x (the stoichiometry was not defined, x is roughly 1.2 here) compound coated on a silicon nitride (SiN) membrane is being used here. The membranes were obtained from Norcada Inc. and the coating was performed by Micromatter Technologies Inc. The nominal thickness of the silicon nitride backing foil was 1000 nm and the nominal mass thickness of the InS_x coating is 151 $\frac{\mu g}{cm^2}$.

The fluorescence and transmission experiments were performed in a photon energy range from below the sulfur K-shell (about 2.1 keV) up to 10 keV using the four-crystal monochromator beamline of PTB at the BESSYII electron storage ring [23]. The tabulated K-shell absorption edge energy for sulfur is 2.472 keV [24]. The experiments were performed out employing an in-house built vacuum chamber [25] equipped with both calibrated photodiodes and an energy-dispersive silicon drift detector (SDD). In addition to the radiometrically calibrated detection efficiency [26], also the SDD's response functions were determined experimentally. The employed SDD is a window-less commercial Bruker detector with an energy resolution at the S-Kα line of about 80 eV (full width at half maximum). Both the sample and a blank silicon nitride foil of identical nominal thickness (for substraction of the silicon nitride transmittance contribution) was aligned into the center of the experimental chamber using an x-y scanning stage. The incident angle θ_{in} between the sample surface and the incident beam was set to 45°.

The recorded fluorescence spectra are then deconvoluted employing the detector response functions for the relevant fluorescence lines including the sulfur Kα and Kβ lines as well as spectral background contributions in order to reliably derive the detected events for the sulfur K-shell fluorescence lines in this case. A fluorescence spectrum recorded at an incident photon energy of 6 keV is shown in figure 1 together with a modeled spectrum based on these contributions.

In general, an experimental determination of FPs for the K-shell of sulfur should provide access to the Kα and Kβ transition probabilities, the K-shell fluorescence yield ω_{F}, the K-shell fluorescence production cross section (FPCS) $\sigma_{\mathrm{K}}(E_0)$ and the K-shell photoionization cross section $\tau_{\mathrm{K}}(E_0)$. In addition, one can calculate the K-shell auger yield ω_{A} using the derived K-shell fluorescence yield ω_{F} as $\omega_{\mathrm{A}} + \omega_{\mathrm{F}} = 1$. The mass attenuation coefficient of sulfur cannot easily be derived as a compound coating is being used here. For a determination of these fundamental parameters an adopted scheme of the recently presented holistic FP determination approach [19] is being used and described in the following. In contrast to the typical data evaluation scheme, it uses a significantly extended studied photon energy range and a novel combined data evaluation scheme

$$\sigma_{\mathrm{K}}\left(E_0\right)\rho d = \omega_{\mathrm{F}}\tau_{\mathrm{K}}\left(E_0\right)\rho d = \frac{\Phi_i^d\left(E_0\right)M_{i,E_0}}{\Phi_0\left(E_0\right)\frac{\Omega}{4\pi}} \tag{1}$$

with

$$M_{i,E_0} = \frac{\left(\frac{\mu_S(E_0)\rho d}{\sin\theta_{\mathrm{in}}} + \frac{\mu_S(E_i)\rho d}{\sin\theta_{\mathrm{out}}}\right)}{\left(1 - \exp\left[-\left(\frac{\mu_S(E_0)\rho d}{\sin\theta_{\mathrm{in}}} + \frac{\mu_S(E_i)\rho d}{\sin\theta_{\mathrm{out}}}\right)\right]\right)}, \tag{2}$$

where θ_{in} and θ_{out} are incident and exit angles, respectively. The incident photon flux $\Phi_0(E_0)$, the sample specific attenuation correction factor M_{i,E_0}, the solid angle of detection $\frac{\Omega}{4\pi}$ and the recorded fluorescence photon flux $\Phi_i^d(E_0)$ need to be derived from the experimental data. For the latter, the deconvoluted detected events for the sulfur K-shell fluorescence lines F_{Ei} must be normalized employing the integration time of each spectrum t_{int} and the detection efficiency the the respective photon energy of each fluorescence line $\epsilon(E_i)$ to derive the fluorescence photon flux $\Phi_i^d(E_0)$. The mass thickness of the sample (product of density ρ

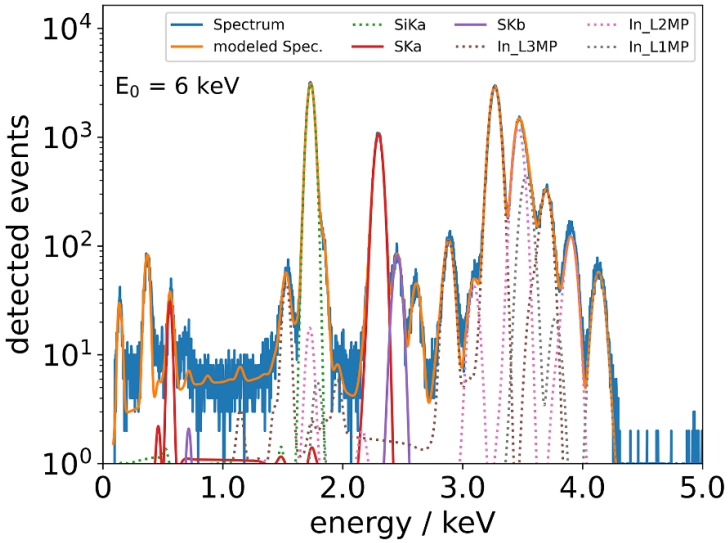

Figure 1. Exemplary fluorescence spectrum recorded on the InS_x coated SiN foil at an incident photon energy of 6 keV. The different relevant detector response functions employed for the spectral deconvolution are also shown.

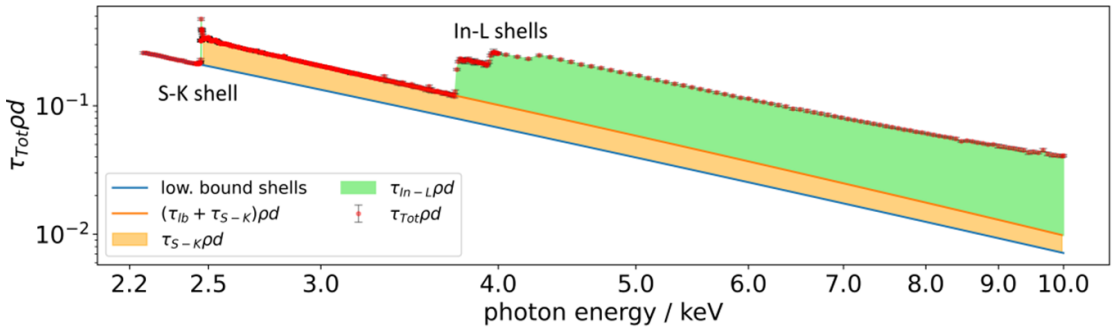

Figure 2. The total sample specific photoionization cross section $\tau_{\mathrm{Tot}}(E_0)\rho d$, which is derived from the transmission data as described in the text, as well as its separation into the various contributions is shown (see text for further details).

and thickness d of the InS_x coating) does not need to be known for a determination of the fluorescence yield. Only the sample specific data as the products of $\tau_{\mathrm{K}}(E_0)$ and $\mu_S(E_0)$ with ρd are required and can be derived directly from the recorded sample transmission data. The incident photon flux $\Phi_0(E_0)$ and the solid angle of detection $\frac{\Omega}{4\pi}$ are also either measured using calibrated photodiodes or are known due to the use of calibrated apertures within the instrumentation [27].

The sample specific attenuation correction factor M_{i,E_0} for the incident (E_0) as well as the fluorescence radiation (E_i) is calculated using equation (2) where the sample specific attenuation coefficients $\mu_S(E_0)\rho d$ and $\mu_S(E_i)\rho d$ are derived from the transmission experiments using the Beer–Lambert law. Thus, M_{i,E_0} is then independent from any database values for mass attenuation coefficients. The sample specific photoionization cross section $\tau_{\mathrm{K}}(E_0)\rho d$ can also be determined from the transmission experiment by subtracting the scattering contributions using to equation (3) (employing the ratio of coherent $\sigma_{C,\mathrm{InS}x}(E_0)$ and incoherent scattering cross sections $\sigma_{I,\mathrm{InS}x}(E_0)$ and tabulated mass attenuation coefficients $\mu_{\mathrm{InS}x}(E_0)$ from X-raylib [24]) and a separation of the total photoionization cross section $\tau_{\mathrm{Tot}}(E_0)\rho d$ into the lower bound subshell contributions of InS_x, the K-shell of sulfur (yellow shaded area) and the contributions from the In-L subshells (green shaded area) as shown in figure 2

$$\tau_{\mathrm{Tot}}(E_0)\,\rho d = \mu_S(E_0)\,\rho d - \frac{\sigma_{C,\mathrm{InS}x}(E_0) + \sigma_{I,\mathrm{InS}x}(E_0)}{\mu_{\mathrm{InS}x}(E_0)}. \tag{3}$$

The separation of $\tau_{\mathrm{Tot}}(E_0)\rho d$ into the relevant partial subshell contributions is realized by scaling Ebel polynomials [28] into the transmission dataset. These polynomials are exponential functions of the form:

$$\tau_{i,E} = \exp\left[A_0 + \ln(E)A_1 + \ln(E)^2 A_2 + \ln(E)^3 A_3 + \ln(E)^4 A_4 + ln(E)^5 A_5\right]. \tag{4}$$

The A_i are modified during the scaling into the experimental $\tau_{\mathrm{Tot}}(E_0)\rho d$ dataset.

Similarly as in the holistic FP determination for L-subshell parameters [19, 20], a much larger transmission and fluorescence dataset with excitation energies far above the sulfur K-shell is used. For the holistic approach, the separation of the sample specific photoionization cross section into the different relevant contributions is performed within an optimization procedure together with the calculation of a sulfur K-shell fluorescence yield employing equation (1) at each probed photon energy above the respective ionization threshold. Using the mean value of these derived fluorescence yields, one can also solve the same equation for the sulfur K-shell $\tau_{\mathrm{K}}(E_0)\rho d$. Then, one can employ the information that the K-shell fluorescence yield should not vary with photon energy, that the transmission and the fluorescence derived $\tau_{\mathrm{K}}(E_0)\rho d$ should match and of course that the summation of the various scaled subshell components must describe the measured total $\tau_{\mathrm{Tot}}(E_0)\rho d$ for an optimizer to find the best solution. Here, a Markov-Chain-Monte-Carlo [29] algorithm is used and the A_i of equation (4) are variable parameters.

This optimization requires two parameters for scaling the contribution of the lower bound shells of InS_x into the dataset. For the sulfur K-shell contribution, at least one parameter (A_0) and up to six parameters (A_0–A_5) can be varied during the optimization. If more degrees of freedom are used, the photon energy dependent decay of the sulfur K-shell contribution can be adjusted whereas if only A_0 is varied, only the magnitude but not the energy dependence can be changed. Parameters of the Ebel polynomial that are not varied are kept fixed to the values found in Ebel's dataset for the sulfur K-shell.

3. Results and discussion

3.1. Determination of the Kα-Kβ ratio

From the experiments performed, the transition probabilities for the sulfur Kα and the sulfur Kβ line by taking into account both the self-attenuation of the sample and the different detection efficiencies of the SDD detector were derived. As the photon energy differences between the Kα_1 and Kα_2 lines and the Kβ_1 and Kβ_3 lines are too small to be distinguishable for such typical energy dispersive x-ray fluorescence spectrometers, only the summed transition probabilities ($\mathrm{K}\alpha = \mathrm{K}\alpha_1 + \mathrm{K}\alpha_2$) for these transitions were determined. In addition, the Kβ to Kα line ratio for sulfur is calculated using the results. These results are shown in figure 3 in comparison to available data from different literature sources.

Here it should be noted, that there may be minor influences of the chemical state the sulfur is present in on the actual Kβ and thus also the Kβ to Kα line ratio. However, the expected effects are small compared to the present uncertainties of the derived transition probabilities [37] and cannot be resolved employing typical energy dispersive detectors such as SDD's.

In comparison to the available data from literature, the commonly used X-raylib tables [24] show best agreement to this work's result. Small deviations are present for both transition probabilities but they agree within the stated uncertainty. Also the other available experimental works on the Kβ to Kα line ratio show reasonable good agreement. The data by Zschornack [30] agrees less good to our data, but this may be influenced by the fact that it was digitized from a graph only. Elam's tabulated data [31] provides incorrect line ratios and transition probabilities for the sulfur K-shell.

3.2. Determination of the K-shell fluorescence yield

The sulfur K-shell fluorescence yield determined in this work is shown in the left panel of figure 4. The uncertainty regime of our result is depicted by the grey shaded area. From comparison to the different available values from literature sources, a good agreement to the experimental work by Haas [38] is found. Agreement within our stated uncertainty range was also found for the commonly used values from X-raylib [24] and the compilations by Bambynek [39] and Kahoul *et al* [40]. The more recent experimental results by Sahin *et al* [36] and Aylikci *et al* [41] are both lower than our result but agree considering the uncertainties. The theoretical calculations by Kostroun *et al* [42] and McGuire [43] fall outside our results, with Kostroun's value being too low and McGuire's too high, even within the uncertainty range.

The also widely used value by Krause [10] is also lower than our result, but it is still within our stated uncertainty. But more importantly, Krause's estimated uncertainty, which is often the only existing guidance for such tabulated data, is significantly larger than our uncertainty budget. This will result also in lower uncertainties in any quantitative x-ray fluorescence result using these fundamental parameters as their uncertainties are usually the dominating contributions.

As the sum of the K-shell fluorescence yield and the K-shell Auger yield is unity, the latter can also be calculated using the determined fluorescence yield result. The thereby determined sulfur K-shell auger yield is shown in the right panel of figure 4. Of course it agrees well with the corresponding value from X-raylib [24] whereas the value derived from Zschornack [30] is slightly higher than our result. But this may be affected by the fact that the Zschornack-result is based on a manual digitization of a plot.

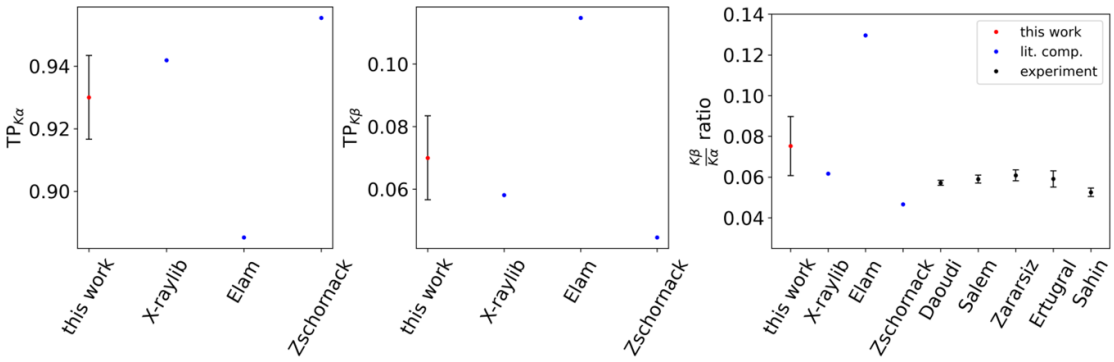

Figure 3. Comparison of the determined fluorescence line ratio between the sulfur K-β and K-α line as well as the transition probabilities of these fluorescence lines with data from various available other works [24, 30–36].

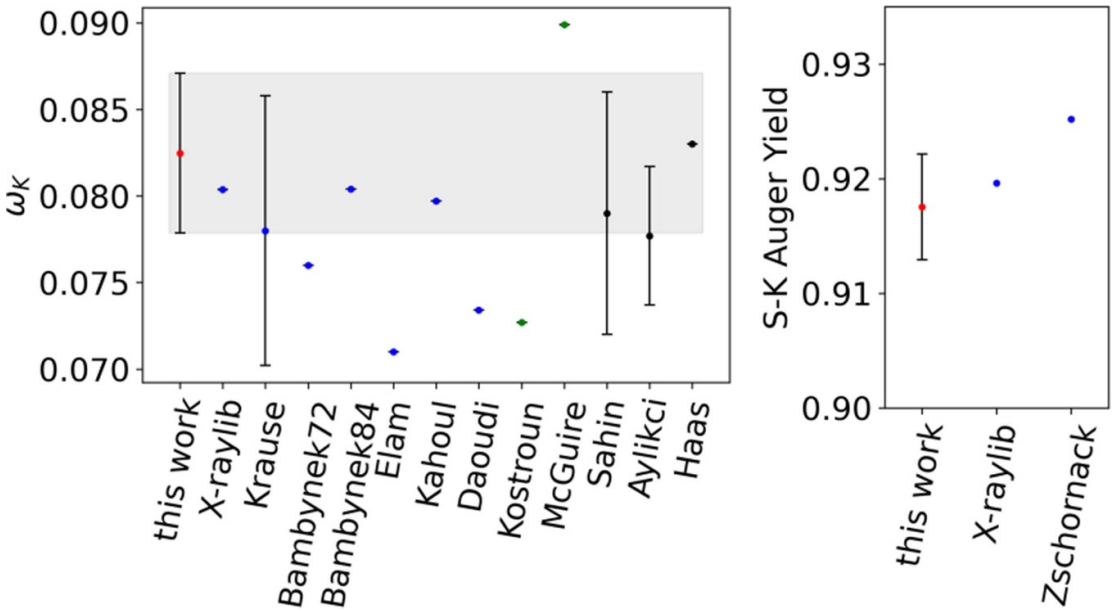

Figure 4. The left panel shows the sulfur K-shell fluorescence yield determined in this work compared with the values from the literature. Data from compilations (blue): [10, 24, 31, 39, 40, 44, 45], theoretically calculated values (green) [42, 43], experimental values (black): [36, 38, 41]. The right panel shows the resulting auger yield for the sulfur K-shell in comparison to data from X-raylib [24] and Zschornack [30].

3.3. Determination of the K-shell fluorescence production cross section

Using equation (1), one can calculate the sample specific FPCSs for sulfur K-shell fluorescence radiation. By taking into account the sample's areal mass of sulfur, the absolute FPCS for S-K fluorescence radiation is calculated at the studied incident photon energies. The samples areal mass of sulfur is derived by performing a reference-free quantification in the photon energy range between 4 keV and 7 keV. For the quantification, the derived sulfur K-shell fluorescence yield and sulfur K-shell photoionization cross sections from X-raylib [24] were used. Here, overall uncertainties for the areal mass of sulfur in the order of 9% was achieved. This leads to an overall uncertainty of the FPCS of about 14%, which could certainly be reduced by employing another way to determine the sample's relevant areal masses such as precision weighing and area measurement [12].

Although the uncertainties of the FPCS derived in this work are relatively large, the data still allows for the verification and evaluation of commonly used literature data. In figure 5, the experimentally derived FPCS are compared against X-raylib data [24]. As can be seen from both the overlay plot and the ratio on the right side, the agreement between our experimental data and the X-raylib data is very good. Both the absolute values and their photon energy dependence are fully matched. Only in the vicinity of the K-absorption edge our derived FPCS data is larger. This is due to the influence of x-ray absorption fine structure near absorption edges, which depends on the chemical state of sulfur atoms and is therefore difficult to account for in databases like X-raylib.

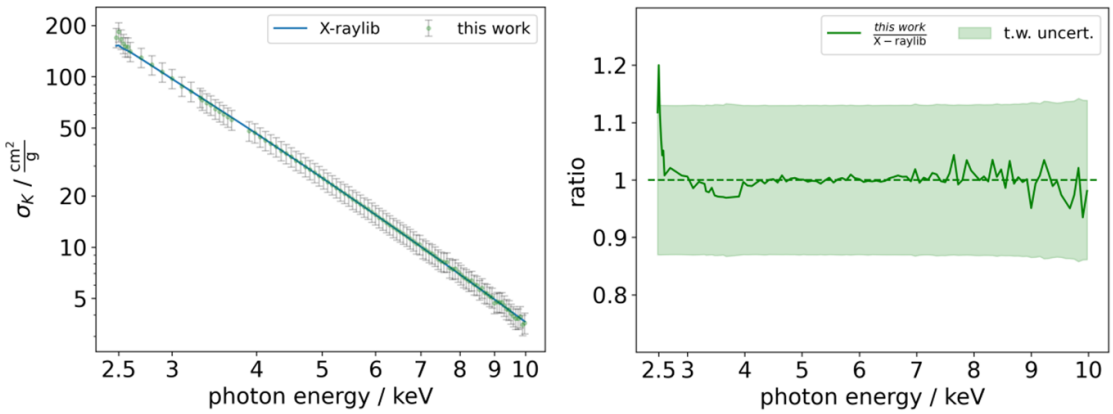

Figure 5. The sulfur K-shell fluorescence production cross section derived in this work compared with the values from X-raylib [24]. On the right side, the ratio of the two datsets is plotted and the green shaded area depicts the uncertainty regime of our data.

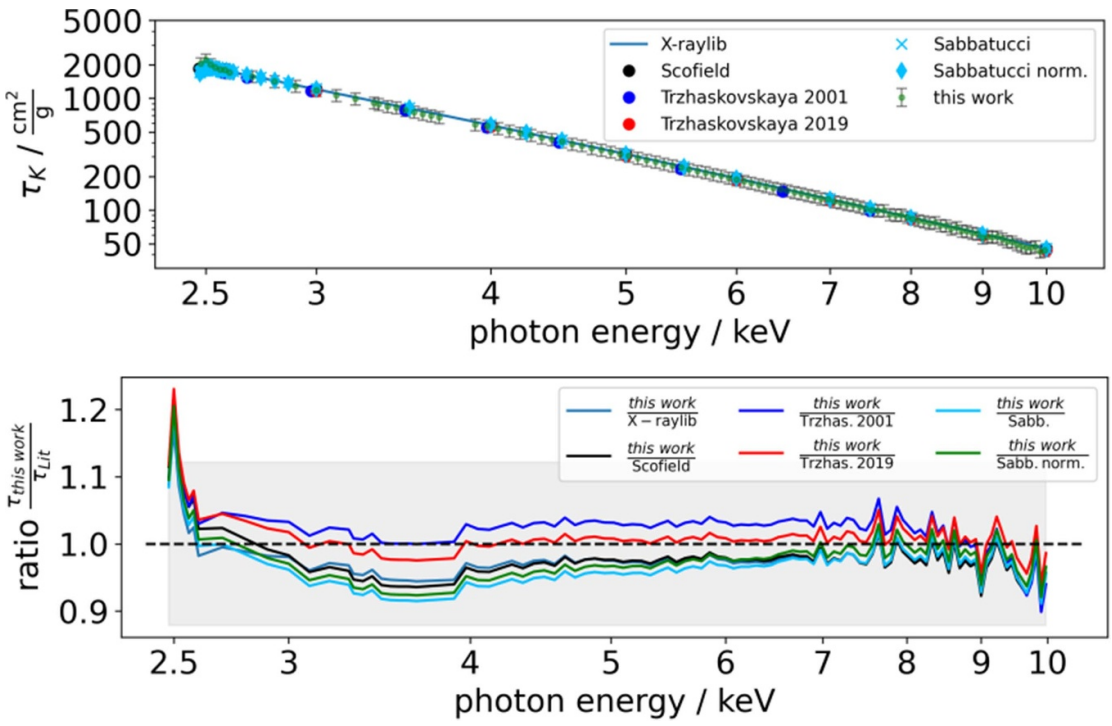

Figure 6. The sulfur K-shell photoionization cross section determined in this work compared with selected values from the literature. Data from X-raylib [24], Scofield [46], Trzhaskovskaya [47, 48] and Sabbatucci [49] are shown.

3.4. Determination of the K-shell photoionization cross section

For the determination of the sulfur K-shell photoionization cross section, also equation (1) is being used. Here, the averaged sulfur K-shell fluorescence yield as presented in section 3.2 is used to calculate the sulfur K-shell photoionization cross section from the experimentally determined FPCSs. For the information on the used sample's areal mass of sulfur, see section 3.3. Of course, also the uncertainties of these cross sections could be lowered if the sulfur areal mass is determined with lower uncertainties.

Nevertheless, a comparison of our determined K-shell photoionization cross section to existing literature data from X-raylib [24] as well as theoretically calculated data by Scofield [46], Trzhaskovskaya [47, 48] and Sabbatucci and Salvat [49] (without and with the screening normalisation correction included) is shown in figure 6. All datasets agree very well with our results except for the very low photon energies in the vicinity of the sulfur K-edge, where chemical species dependent x-ray absorption fine structure may be present in our data. The ratio plots in the lower panel indicate small differences between the datasets and the most recent calculations by Trzhaskovskaya and Yarzhemsky [48] also reproduce the present absolute values very well.

4. Conclusion

The novel holistic approach for the experimental determination of atomic fundamental parameters was applied to sulfur K-shell parameters. The S K-shell fluorescence yield, the transition probabilities of the main K-shell fluorescence lines as well as the FPCSs and the S K-shell photoionization cross sections have been determined in this work. All results are also downloadable from Zenodo as plain text [21].

In contrast to our recent works on L-subshell fundamental parameter determinations [19, 20], the application of the holistic approach does not yield significant uncertainty reduction as compared to the former experimental approach [50] in the case of K-shell parameters. But this is more due to the fact, that the achieveable uncertainties for e.g. the K-shell fluorescence yield were already quite low also with the classic experimental determination scheme. As there are no Coster-Kronig factors and only one absorption edge, the whole FP determination procedure is much less complex at the K-shell as compared to the L-subshells. However, the achieved uncertainty is lower than the Krause estimates [10], especially for lighter elements and the application of the holistic approach enables the determination of the fluorescence production—and the K-shell photoionization cross sections in a broad photon energy regime.

In general, a good agreement between fundamental parameter data from the X-raylib compilation [24] and our results for the whole set of determined parameters was found. This aligns with earlier findings for other elements and shells, demonstrating the quality of the X-raylib table. Nevertheless, the present result allow for a more solid assessment of the uncertainties of the tabulated data. Especially the FPCS agrees very well with our result and thus the uncertainty of X-raylib data can be assumed to be rather low. This will allow to reduce also the quantification uncertainties when using this data for FP-based quantification algorithms, e.g. for the already mentioned quantitative operando LiS battery studies.

Data availability statement

The data that support the findings of this study are openly available at the following URL/DOI: https://zenodo.org/records/12622658.

Acknowledgments

This project has received funding from the ECSEL Joint Undertaking (JU) IT2 under Grant Agreement No. 875999. The JU receives support from the European Union's Horizon 2020 research and innovation program and the Netherlands, Belgium, Germany, France, Austria, Hungary, the United Kingdom, Romania and Israel. This work was also supported by the European Partnership on Metrology, co-financed by the European Union's Horizon Europe Research and Innovation Programme and by the Participating States through Grant Agreement 21GRD01 (OpMetBat).

ORCID iD

Philipp Hönicke https://orcid.org/0000-0002-0712-903X

References

[1] Prakash Narayan O, Kumar P, Yadav B, Dua M and Kumar Johri A 2022 Sulfur nutrition and its role in plant growth and development *Plant Signal. Behav.* **18** 2030082
[2] Feng M, Tang B, Liang S H and Jiang X 2016 Sulfur containing scaffolds in drugs: synthesis and application in medicinal chemistry *Curr. Top. Med. Chem.* **16** 1200–16
[3] McGorrin R J 2011 *The Significance of Volatile Sulfur Compounds in Food Flavors: An Overview* (American Chemical Society) pp 3–31
[4] Kato H, Nakatsubo F, Abe K and Yano H 2015 Crosslinking via sulfur vulcanization of natural rubber and cellulose nanofibers incorporating unsaturated fatty acids *RSC Adv.* **5** 29814–9
[5] Teng Y, Zhou Q and Gao P 2019 Applications and challenges of elemental sulfur, nanosulfur, polymeric sulfur, sulfur composites and plasmonic nanostructures *Crit. Rev. Environ. Sci. Technol.* **49** 2314–58
[6] Su Y-S and Manthiram A 2012 Lithium–sulphur batteries with a microporous carbon paper as a bifunctional interlayer *Nat. Commun.* **3** 1166
[7] Cheng W, Zhao M, Lai Y, Wang X, Liu H, Xiao P, Mo G, Liu B and Liu Y 2023 Recent advances in battery characterization using in situ XAFS, SAXS, XRD and their combining techniques: from single scale to multiscale structure detection *Exploration* **4** 20230056
[8] Zech C, Hönicke P, Kayser Y, Risse S, Grätz O, Stamm M and Beckhoff B 2021 Polysulfides driven degradation in lithium-sulfur batteries during cycling—quantitative and high time-resolution operando x-ray absorption study for dissolved polysulfides probed at both electrode sides *J. Mater. Chem.* A **9** 10231–9
[9] Doyle A, Saavedra A, Tristão M L B and Aucelio R Q 2015 Determination of S, Ca, Fe, Ni and V in crude oil by energy dispersive x-ray fluorescence spectrometry using direct sampling on paper substrate *Fuel* **162** 39–46
[10] Krause M O 1979 Atomic radiative and radiationless yields for K and L shells *J. Phys. Chem. Ref. Data* **8** 307–27

[11] 2021 International initiative on x-ray fundamental parameters (available at: www.exsa.hu/fpi.php) (Accessed 3 June 2022)
[12] Ménesguen Y, Lépy M C, Hönicke P, Unterumsberger R Müller M, Beckhoff B, Hoszowska J and Dousse J-C 2017 Experimental determination of x-ray atomic fundamental parameters of nickel *Metrologia* **55** 56
[13] Guerra M, Sampaio J M, Parente F, Indelicato P, Hönicke P, Müller M, Beckhoff B, Marques J P and Santos J P 2018 Theoretical and experimental determination of K- and L-shell x-ray relaxation parameters in Ni *Phys. Rev.* A **97** 042501
[14] Baptista G, Pinheiro D, Machado J, Guerra M, Amaro P and Paulo Santos J 2024 Lisbon atomic database (LISA): a compilation of calculated fundamental atomic parameters *Eur. Phys. J.* D **78** 18
[15] Beckhoff B 2022 Traceable characterization of nanomaterials by x-ray spectrometry using calibrated instrumentation *Nanomaterials* **12** 2255
[16] Hönicke P, Kolbe M and Beckhoff B 2016 What are the correct L-subshell photoionization cross sections for quantitative X-Ray spectroscopy? *X-Ray Spectrom.* **45** 207–11
[17] Hönicke P, Kolbe M, Krumrey M, Unterumsberger R and Beckhoff B 2016 Experimental determination of the oxygen k-shell fluorescence yield using thin SiC_2 and Al_2O_3 foils *Spectrochim. Acta* B **124** 94–98
[18] Kayser Y, Hönicke P, Wansleben M, Wählisch A and Beckhoff B 2022 Experimental determination of the gadolinium L subshells fluorescence yields and Coster-Kronig transition probabilities *X-Ray Spectrom.* **52** 235-246
[19] Hönicke P 2023 A novel and holistic approach for experimental x-ray fundamental parameter determination—the Ru L-shell *New J. Phys.* **25** 073012
[20] Wauschkuhn N, Gundlach H and Hönicke P 2024 Experimental determination of the hafnium L-subshell fundamental parameters using the holistic approach *New J. Phys.* **26** 033017
[21] Hönicke P 2024 Experimental determination of the sulfur K-shell fundamental parameters employing the holistic approach *Zenodo* (available at: https://10.5281/zenodo.12622657)
[22] Nordfors B 1960 The statistical errors in x-ray absorption measurements *Ark. Fys.* **18** 37–47
[23] Krumrey M and Ulm G 2001 High-accuracy detector calibration at the PTB four-crystal monochromator beamline *Nucl. Instrum. Meth.* A **467–468** 1175–8
[24] Schoonjans T, Brunetti A, Golosio B, Sanchez del Rio M, Solé V A, Ferrero C and Vincze L 2011 The xraylib library for x-ray–matter interactions. recent developments *Spectrochim. Acta* B **66** 776–84
[25] Kolbe M, Beckhoff B, Krumrey M and Ulm G 2005 Thickness determination for Cu and Ni nanolayers: comparison of reference-free fundamental-parameter based x-ray fluorescence analysis and x-ray reflectometry *Spectrochim. Acta* B **60** 505–10
[26] Scholze F and Procop M 2009 Modelling the response function of energy dispersive x-ray spectrometers with silicon detectors *X-Ray Spectrom.* **38** 312–21
[27] Beckhoff B 2008 Reference-free x-ray spectrometry based on metrology using synchrotron radiation *J. Anal. At. Spectrom.* **23** 845–53
[28] Ebel H, Svagera R, Ebel M F, Shaltout A and Hubbell J H 2003 Numerical description of photoelectric absorption coefficients for fundamental parameter programs *X-Ray Spectrom.* **32** 442–51
[29] Foreman-Mackey D, Hogg D W, Lang D and Goodman J 2013 emcee: the MCMC hammer *Publ. Astron. Soc. Pac.* **125** 306–12
[30] Zschornack G H (ed) 2007 *Handbook of X-ray Data* (Springer)
[31] Elam W T, Ravel B D and Sieber J R 2002 A new atomic database for x-ray spectroscopic calculations *Rad. Phys. Chem.* **63** 121–8
[32] Daoudi S, Kahoul A, Kup Aylikci N, Sampaio J M, Marques J P, Aylikci V, Sahnoune Y, Kasri Y and Deghfel B 2020 Review of experimental photon-induced $\frac{K\beta}{K\alpha}$ intensity ratios *At. Data Nucl. Data Tables* **132** 101308
[33] Salem S I, Falconer T H and Winchell R W 1972 $\frac{K\beta}{K\alpha}$ radiative-transition-probability ratios for elements of low atomic numbers in amorphous and crystal forms *Phys. Rev.* A **6** 2147–50
[34] Zararsiz A 1994 $\frac{K\beta}{K\alpha}$ x-ray intensity ratio in the region of $15 \leqslant z \leqslant 22$ *J. Radioanal. Nucl. Chem. Art.* **185** 193–7
[35] Ertuğral B, Apaydın G, Çevik U, Ertuğrul M and Kobya A 2007 $\frac{K\beta}{K\alpha}$ x-ray intensity ratios for elements in the range $16 \leqslant z \leqslant 92$ excited by 5.9, 59.5 and 123.6 kev photons *Radiat. Phys. Chem.* **76** 15–22
[36] Şahin M, Demir L and Budak G 2005 Measurement of K x-ray fluorescence cross-sections and yields for 5.96kev photons *Appl. Radiat. Isot.* **63** 141–5
[37] Mukoyama T, Taniguchi K and Adachi H 1986 Chemical effect on $\frac{K\beta}{K\alpha}$ x-ray intensity ratios *Phys. Rev.* B **34** 3710–6
[38] Haas M 1933 Der nutzeffekt der röntgen-k-fluoreszenzstrahlung bei leichten elementen *Ann. Phys., Lpz.* **408** 473–88
[39] Bambynek W 1984 New evaluation of K-fluorescence yields *X-ray and Inner-Shell Processes in Atoms, Molecules and Solids, Post-Deadline Abstracts* p 1
[40] Kahoul A, Aylikci V, Kup Aylikci N, Cengiz E and Apaydın G 2012 Updated database and new empirical values for K-shell fluorescence yields *Rad. Phys. Chem.* **81** 713–27
[41] Aylıkcı V, Cengiz E, Apaydın G, Ünver Y, Sancak K and Tıraşoğlu E 2008 Influence of functional group effect on the K-shell x-ray production cross-sections and average fluorescence yields of sulphur in 1,2,4-triazol-5-one compounds containing thiophene *Chem. Phys. Lett.* **461** 332–7
[42] Kostroun V O, Chen M H and Crasemann B 1971 Atomic radiation transition probabilities to the 1s state and theoretical k-shell fluorescence yields *Phys. Rev.* A **3** 533–45
[43] McGuire E J 1970 K-shell auger transition rates and fluorescence yields for elements ar-xe *Phys. Rev.* A **2** 273–8
[44] Bambynek W, Craseman B, Fink R W, Freund H-U, Mark H, Swift C D, Price R E and Venugopala Rao P 1972 X-ray fluorescence yields, auger and coster-kronig transistion probabilities *Rev. Mod. Phys.* **44** 716–813
[45] Daoudi S, Kahoul A, Sahnoune Y, Deghfel B, Kasri Y, Khalfallah F, Aylikci V, Aylikci N K, Medjadi D E and Nekkab M 2015 New K-shell fluorescence yields curve for elements with $3 \leqslant z \leqslant 99$ *J. Korean Phys. Soc.* **67** 1537–43
[46] Scofield J H 1973 Theoretical photoionisation cross sections from 1 to 1500 keV *UCRL Report* 51326 (Lawrence Livermore Laboratory, USA)
[47] Trzhaskovskaya M B, Nefedov V I and Yarzhemsky V G 2001 Photoelectron angular distribution parameters for elements $z = 1$ to $z = 54$ in the photo electron energy range 100 eV to 5000 eV *At. Data Nucl. Data* **77** 97–159
[48] Trzhaskovskaya M B and Yarzhemsky V G 2019 Dirac-Fock photoionization parameters for HAXPES applications, part II: inner atomic shells *At. Data Nucl. Data Tables* **129-130** 101280
[49] Sabbatucci L and Salvat F 2015 Theory and calculation of the atomic photoeffect *Radiat. Phys. Chem.* **121** 122–40
[50] Kolbe M and Hönicke P 2015 Fundamental parameters of Zr and Ti for a reliable quantitative x-ray fluorescence analysis *X-Ray Spectrom.* **44** 217–20